



ELSEVIER

Polymer 43 (2002) 6805–6811

**polymer**

[www.elsevier.com/locate/polymer](http://www.elsevier.com/locate/polymer)

# The effect of filler type, morphology and coating on the anisotropy and microstructure heterogeneity of injection-moulded discs of polypropylene filled with aluminium and magnesium hydroxides. Part 1. A wide-angle X-ray diffraction study

J.I. Velasco<sup>a,\*</sup>, C. Morhain<sup>a</sup>, A.B. Martínez<sup>a</sup>, M.A. Rodríguez-Pérez<sup>b</sup>, J.A. de Saja<sup>b</sup>

<sup>a</sup>Centre Català del Plàstic, Universitat Politècnica de Catalunya, C. Colom 114, Terrassa, Barcelona 08222, Spain

<sup>b</sup>Departamento de Física de la Materia Condensada, Cristalografía y Mineralogía, Facultad de Ciencias, Universidad de Valladolid, Prado de la Magdalena s/n, 47011 Valladolid, Spain

Received 25 March 2002; received in revised form 30 May 2002; accepted 13 September 2002

## Abstract

The influence of aluminium hydroxide particle morphology and magnesium hydroxide surface coating on the anisotropy and microstructure heterogeneity of injection-moulded discs of polypropylene (PP) filled with 40% by weight of these fillers has been studied through wide-angle X-ray diffraction measures. In general, the discs displayed an anisotropic structure due to different orientations of both filler particles and PP crystals through the part thickness. The samples also exhibited some degree of heterogeneity due to different levels of particle orientations in specimens far away and close to the disc mould entrance. © 2002 Elsevier Science Ltd. All rights reserved.

**Keywords:** Polypropylene; Flame retardant fillers; Injection-moulding; Anisotropy; Wide-angle X-ray diffraction

## 1. Introduction

Polypropylene is probably the most-used mineral-filled thermoplastic polymer for injection moulding applications [1]. Incorporation of plate-like mineral fillers (talc, mica, etc.) into thermoplastics is well established and has been studied extensively [2–6]. In injection-moulded parts both polymer molecules and anisometric filler particles can remain highly oriented due to the high shear rates involved [7]. If localised cooling rates are sufficiently rapid to render the orientation effects permanent, the degree and distributions of polymer crystals and particle alignment become highly significant, since they are important determinants of subsequent physical properties such as elastic modulus, anisotropic shrinkage and part distortion. A considerable gradient of both filler particles and polymer orientation may be formed through the thickness of the part and, frequently, it is possible to identify several layers through the section comprising two outer skins and the core. As a consequence, the interior structure is far from being homogeneous or

isotropic [8,9] and it is remarkably dependent on the moulding conditions. Moreover, additional complexities are created by the presence of filler coatings [10]. Although their principal function is to enhance particle dispersion by reducing the work of adhesion between filler and matrix [11], most coatings also modify the rheological behaviour of the compound. In this sense, the importance of wall-slip phenomena has been pointed-out with respect to the shear-induced alignment of both molecular chains and anisometric filler particle [12].

The structure of injection-molded filled PP composites is especially stimulating due to the induced crystalline structure that PP presents when is processed in the presence of mineral fillers, which can act as nucleating agents for the polymer. Consequently, the PP phase in the composites could also present anisotropic properties.

Keeping the previous notions in mind and following early investigations on these topics [13–15], the goal of the present work has been the characterisation of the anisotropy and the microstructural heterogeneity of injection-moulded discs of magnesium hydroxide and aluminium hydroxide filled polypropylene, as well as, the analysis of the influence

\* Corresponding author. Tel.: +34-93783-7022; fax: +34-93784-1827.  
E-mail address: jose.ignacio.velasco@upc.es (J.I. Velasco).

of the filler type, morphology and coating. This has been carried out by means of wide-angle X-ray diffraction (WAXD) measures. Furthermore, thermal and dynamic mechanical behaviours have also been studied in these samples and related to the anisotropy and heterogeneity. These results are to be appeared in a separated paper [15].

## 2. Materials, compounding and specimens

A commercial grade of polypropylene homopolymer (Isplen PP050), supplied by Repsol Química S.A., was used in this work. Magnesium hydroxide, employed as filler, was a high purity untreated grade (Magnifin H5) supplied by Martinswerk GmbH. The average particle size was  $1.5 \mu\text{m}$  and the specific surface area  $5.0 \text{ m}^2/\text{g}$ . Two commercial grades of surface-coated  $\text{Mg}(\text{OH})_2$  were also studied. These were Magnifin H5L and H5KV. Infrared spectroscopy (FTIR) analysis revealed that the coatings were based on poly(ethylene: vinyl acetate) and poly(dimethylsiloxane), respectively. The hexagonal platy morphology of the  $\text{Mg}(\text{OH})_2$  particles can be appreciated in Fig. 1. Martinswerk GmbH also kindly supplied two uncoated aluminium hydroxide grades (Martinal ON and OL-104-LE), which morphologies are shown in Fig. 1(d) and (e). The ON filler had irregular, approximately spherical particles with an average diameter of  $60 \mu\text{m}$  and a specific surface area of  $0.5 \text{ m}^2/\text{g}$ , whereas the OL grade had a mean particle diameter of  $1.5 \mu\text{m}$  and a specific surface area of  $3.1 \text{ m}^2/\text{g}$ . The OL grade notwithstanding had a small fraction of hexagonal platy particles.

To prepare and characterise materials that could have some degree of flame retardancy, moderate filler concentrations (40% by weight) were used to produce the samples.

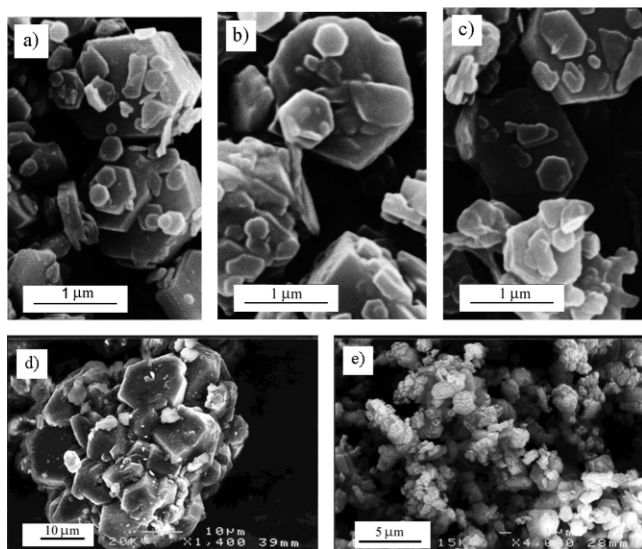


Fig. 1. Morphology of the fillers observed by SEM. (a)  $\text{Mg}(\text{OH})_2$  particles H5, (b)  $\text{Mg}(\text{OH})_2$  particles H5L, (c)  $\text{Mg}(\text{OH})_2$  particles H5KV, (d)  $\text{Al}(\text{OH})_3$  particles ON, (e)  $\text{Al}(\text{OH})_3$  particles OL.

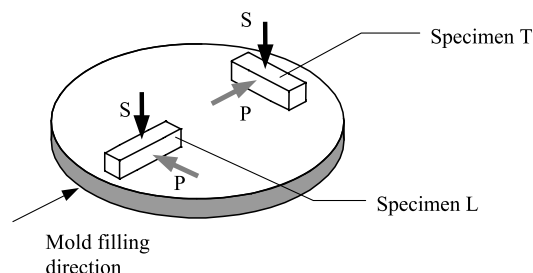


Fig. 2. Specimens and testing directions in the injection-moulded discs.

Therefore, PP was filled with 40% nominal concentrations by weight of  $\text{Mg}(\text{OH})_2$  and  $\text{Al}(\text{OH})_3$ . Compounding was performed using a *Collin* co-rotating twin-screw extruder of 25-mm screw diameter and a length of 600 mm. A good dispersion of the filler particles into the PP matrix was achieved with the following screw configuration: two compression zones on both sides of a mixing zone constituted by double-tipped kneading elements. Typical screw speed was 80–100 rpm and the temperature profile selected was from  $160 \text{ }^\circ\text{C}$  at the polymer entrance to  $185 \text{ }^\circ\text{C}$  at the die. The melt temperature measured at the die was never higher than  $195 \text{ }^\circ\text{C}$ . A circular cross-section die of diameter 3 mm was employed, and the extrudate was cooled in water and pelletised.

The unfilled PP was also extruded in the same way in order to have similar thermal and mechanical history than that of the filled compounds.

Discs of 78 mm nominal diameter and 4 mm nominal thickness were injection-moulded using a 440/90 injection-moulding machine and a multiple cavity mould, as described in Fig. 4 of the ASTM D-638 standard. The nominal injection pressure was 100 MPa and the temperature of the melt  $195 \text{ }^\circ\text{C}$ . Under these conditions, the shear rate was about  $10^3 \text{ s}^{-1}$ . All the discs were annealed at  $115 \text{ }^\circ\text{C}$  for 24 h, in order to release residual stresses; any deformed specimens were rejected.

From each disc two prismatic bars (Fig. 2) of nominal dimensions  $25 \text{ mm} \times 4 \text{ mm} \times 4 \text{ mm}$  were machined in order to use them as testing specimens to characterise the heterogeneity and anisotropy in these injection-moulded parts. For this purpose, 'L' specimens were cut from the zone of the disk closer to the mould cavity entrance, having its length axis parallel to the main flow direction; 'T' specimens were cut from the opposite zone of the disk with its length axis perpendicular to the main flow direction.

## 3. Testing procedure

### 3.1. Preliminary measurements

Some basic measures were taken on the PP and the different filled materials. The material density was measured through the hydrostatic method. The filler weight concentration in the composites was determined from

Table 1  
Reference, composition and basic characteristics of the samples

Sample	Density (g/cm <sup>3</sup> )	Filler content		Melt flow index (g/10 min)	Volumetric melt flow index (cm <sup>3</sup> /10 min)	Heat deflection temperature (°C)
		Weight fraction	Volume fraction			
PP	0.902	0	0	2.19	2.89	70.3
PPH5	1.181	0.399	0.198	1.74	1.67	115.5
PPH5L	1.181	0.402	0.199	1.94	1.86	83.9
PPH5KV	1.185	0.403	0.200	2.70	2.58	92.5
PPOL	1.166	0.398	0.192	1.50	1.44	116.5
PPON	1.156	0.396	0.189	1.66	1.59	114.2

measurements of weight loss after sample combustion. From the values of density and filler weight fraction, the filler volume fraction could be determined. To have information about the influence of the fillers on the molten-state characteristics of the filled polymer, measures of the melt flow index (MFI) and the volumetric melt flow index (MFI-v) were taken at 190 °C and 2160 g of load. Finally, values of the heat deflection temperature (HDT) were obtained at a heating rate of 2 °C/min applying a three-point-bending stress of 1.8 MPa on injection-moulded prismatic specimens of nominal dimensions 127 × 12.7 × 6.35 mm<sup>3</sup>. The selected span was 100 mm.

### 3.2. Wide-angle X-ray diffraction

The experiments were performed using a *Philips* PW 1050/71 diffractometer. Radial scans of intensity (*I*) versus scattering angle ( $2\theta$ ) were recorded in the range 5–40° at a scanning speed for the detector displacement of 0.020/0.800°/s by using filtered Cu K $\alpha$  radiation. In order to study the anisotropy, the scans were taken from *S* and *P* surfaces in each sample, as shown in Fig. 2.

### 3.3. Scanning electron microscopy (SEM)

A *Jeol*-820 scanning electron microscope was used for the observation of the morphology of the filler particles. Vacuum coating with gold was applied on the samples to promote conductivity.

## 4. Results and discussion

Results of the preliminary measures are shown in Table 1. These indicating that the filler concentration was constant (40% by weight) in all the prepared materials, thus they were accurate samples to analyse filler effects comparatively.

The influence of filler characteristics on the melt viscosity could be analysed with the MFI-v values. Aluminium hydroxide reduced the MFI-v value more than magnesium hydroxide, indicating a higher viscosity increase. The uncoated grade (H5) promoted higher

reduction than the coated ones (H5L and especially H5KV), this indicating that the surface treatments employed have a lubricant effect on the PP. On the other hand, the HDT value was found to be very sensitive to the filler characteristics. As one can be seen in Table 1, remarkable differences were found in HDT values according to the different filler in the sample. As expected, filled samples resulted in higher HDT values than unfilled PP. However, differences up to 25 °C were observed as a result of the different filler surface coatings.

### 4.1. Filler particle and polymer crystal orientations

From the measurements carried out by WAXD, information about orientations of filler particles and polymer were obtained. The Bravais lattice of the main crystalline phase of PP ( $\alpha$  phase) is monoclinic ( $a = 6.65$  Å,  $b = 20.96$  Å,  $c = 6.5$  Å), while the less common PP  $\beta$  phase is hexagonal ( $a = b = 12.74$  Å,  $c = 6.35$  Å). Aluminium hydroxide Bravais lattice is monoclinic ( $a = 8.64$  Å,  $b = 5.07$  Å,  $c = 9.72$  Å), and that of magnesium hydroxide is hexagonal ( $a = b = 3.14$  Å,  $c = 4.77$  Å).

The intensity ratio between the diffraction planes (001) and (101) for magnesium hydroxide (peaks at  $2\theta = 17.4$  and  $37.8^\circ$ , respectively), and  $I(004)/I(110)$  for aluminium hydroxide (peaks at  $2\theta = 37.1$  and  $20.2^\circ$ , respectively) are collected in Table 2 for the different samples and analysis directions. The high values for the LS and TS directions and the low values for the LP and TP ones indicate that the particles are mainly parallel to the surface of the discs in the

Table 2  
Characteristic WAXD intensity ratio of magnesium and aluminium hydroxide

Sample	LS	LP	TS	TP
<i>I</i> (001)/ <i>I</i> (101)				
PPH5	18.808	0.364	33.154	0.296
PPH5L	23.132	0.464	37.125	0.410
PPHKV	42.177	0.482	68.604	0.370
<i>I</i> (004)/ <i>I</i> (110)				
PPOL	1.671	0.116	2.744	1.460
PPON	0.723	0.182	0.887	0.739

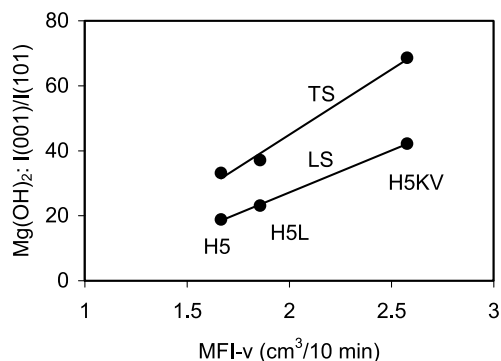


Fig. 3. Intensity ratio  $I(001)/I(101)$  for the  $Mg(OH)_2$  particles as a function of the MFI-v.

skin zone. The values of the intensity ratios are not strictly comparable for both kinds of particles due to the different Bravais lattice in which both crystallise. Nevertheless, the very strong differences between those values seem to indicate that  $Mg(OH)_2$  particles are more oriented parallel to the surface of the injection-moulded part than  $Al(OH)_3$  particles.

The particle morphology seems to have some effect on the orientation. For example, PPON composite, in which polycrystalline aggregates were found, showed lower differences between the parallel orientation to the surface (LS and TS) and the perpendicular one (LP and TP) than those found in the PPOL sample. Particle aggregates did not exist in aluminium hydroxide OL grade (Fig. 1(e)). In this filler, a certain fraction of well-defined hexagonal particles can also be identified.

In general, particle orientation measured in  $S$  direction has been found to be more pronounced in  $T$  specimens than in  $L$  ones, showing this fact that the injected discs are not homogeneous, at least concerning the filler orientation distribution. A possible cause of this effect is the flow restriction that the melt suffers as it progress in the mould cavity, which results in a higher particle orientation degree far from the cavity entrance due to increased shear stresses. This well-known effect is caused by the skin formation in the moulded part due to the melt solidification as it touches the mould surface. In injection-moulded parts, the thickness of the formed skin is larger near to the mould gate than in remote regions.

The  $Mg(OH)_2$  surface treatments used in this work have shown a significant effect on the particle orientation in the moulded part. Particle orientation was higher when lubricant surface coatings were applied. On the one hand, the particle orientation in the PPH5KV composite was the most pronounced; a PDMS-based coating was used in H5KV filler. On the other hand, the particle orientation in PPH5L composite was higher than that in the non-coated material PPH5. The coating given to H5L grade was based on EVA copolymer and, as commented before, this coating acts slightly as a lubricant, reducing the melt viscosity, although the viscosity reduction was found much higher for

Table 3

Characteristic WAXD intensity ratio of polypropylene

Sample	LS	LP	TS	TP
$I(040)/I(110)$				
PP	1.302	1.023	1.016	0.689
PPH5	4.221	0.574	5.065	0.429
PPH5L	1.394	0.977	1.374	0.660
PPHKV	1.362	0.887	1.177	0.642
PPOL	2.062	1.077	2.324	1.060
PPON	1.333	0.856	1.535	0.616

the coating based on PDMS. The orientation degree of the magnesium hydroxide particles in the specimen skin as a function of the MFI-v value is shown in Fig. 3. It is well known that increasing the shear rate induces a more oriented skin [16]. The shear rate at constant pressure during the mould filling depends on the melt viscosity. As expected, as the melt viscosity decreased (MFI-v increased), the orientation of the filler platelets increased.

Focusing the attention on the polymer, the relationship between the orientation of polypropylene  $a$ - and  $b$ -axes was determined by taking the ratio of the intensity of polypropylene (040) plane (peak at  $2\theta = 16.7^\circ$  in the diffraction pattern) to the (110) plane (peak at  $2\theta = 13.9^\circ$ ). Several values of this ratio are found in the literature for an isotropic mixture of PP crystallites (i.e. 0.54 [17] and values comprised between 0.67 and 0.77 [18]). Nevertheless, the morphology and orientation of PP crystals is very dependent on the crystallisation and moulding conditions, and especially on the filler characteristics. The results (Table 3) suggested a higher orientation of the PP crystals in the disc skin. However, these differences were only significant in materials filled with uncoated, low particle size, fillers (i.e. OL and especially H5). Therefore, it can be pointed out, that the coatings used for the  $Mg(OH)_2$  particles reduced the PP crystals orientation. A similar effect was detected when the  $Al(OH)_3$  particle size increases.

The former results seem to indicate that the orientation of the crystalline phase of the polymer is not induced by the orientation of filler particles, but it seems to depend on factors affecting the polymer nucleation rate, such as the filler nature, morphology and particle surface characteristics. These effects can be clearly appreciated in Fig. 4, where both the polymer crystal and the filler particle orientations have been related between themselves for all the samples and analysis directions.

In order to analyse the effect of the particle orientation on the PP crystals orientation, values of the normalised polymer crystal orientation (NCO) parameter for  $Mg(OH)_2$  and  $Al(OH)_3$  filled samples, defined by Eqs. (1) and (2), respectively, have been computed and plotted in Fig. 5.

$$NCO = \frac{(I(040)/I(110))_{\text{filled PP}}}{(I(040)/I(110))_{\text{unfilled PP}}(I(001)/I(101))_{Mg(OH)_2}} \quad (1)$$

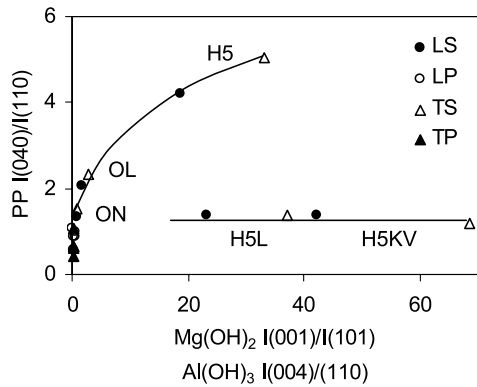


Fig. 4. Intensity ratio  $I(040)/I(110)$  for the PP phase as a function of the characteristic intensity ratio for the fillers.

$$NCO = \frac{(I(040)/I(110))_{\text{filled PP}}}{(I(040)/I(110))_{\text{unfilled PP}}(I(004)/I(110))_{\text{Al(OH)}_3}} \quad (2)$$

The NCO values for the  $Mg(OH)_2/PP$  composites result very low in *S* direction and high in *P* direction. The opposite result is found for PPOL sample. The PPON presents similar values in both directions. This reveals that the aluminium hydroxide particles (especially the OL grade) produce a

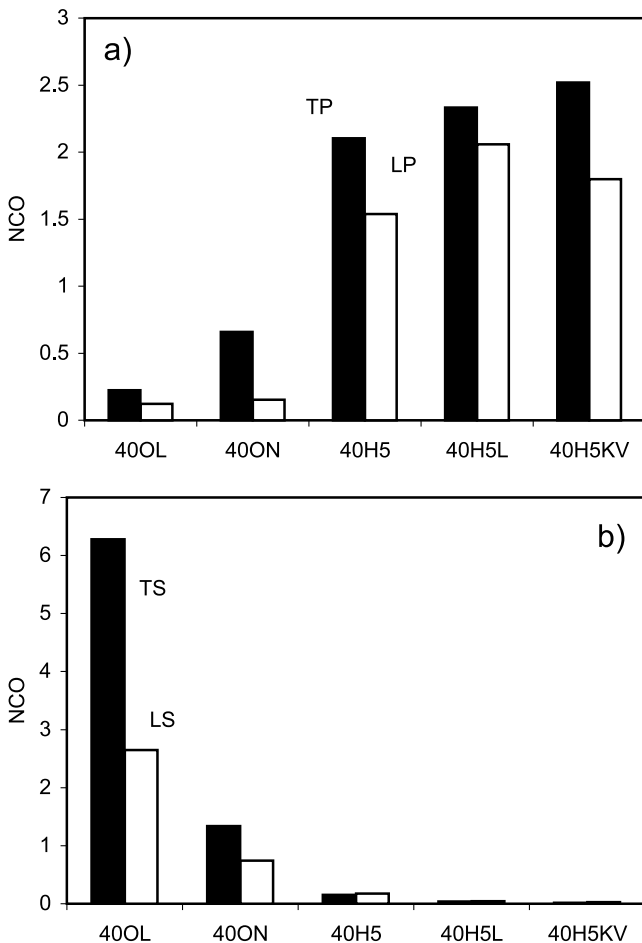


Fig. 5. NCO parameter for all the materials and directions under study. (a) Values in *P* direction. (b) Values in *S* direction.

strong parallel orientation of the PP crystals, independently of their own orientation. For the magnesium hydroxide grades, the previous orientation is lower and independent of the surface treatment.

The values of the NCO parameter were higher for T samples than for L ones. As it was mentioned in the previous discussion, this result is due to the higher particle orientation in the surface of the T samples (Fig. 3).

WAXD experiments also provided information about the presence of the PP  $\beta$ -phase (plane (300) at  $2\theta = 16.3^\circ$ ) in the studied samples. As shown in Table 4, this crystalline phase appeared only in L specimens of pure PP and in specimens (L and T) of materials filled with surface-coated  $Mg(OH)_2$ .

The main aspects involved in the nucleation and crystallisation of  $\beta$ -phase in PP have been studied by Varga [19], and it has been established that this kind of crystallisation appears for temperatures below  $140^\circ C$  approximately. For filled polymers in which the filler acts as a nucleating agent and at temperatures above the previous critical value the polymer mainly crystallises in the  $\alpha$ -modification. In addition, high shear stresses could promote PP  $\beta$ -phase formation. Furthermore, although it has been suggested [20] that uncoated fillers can induce the PP  $\beta$ -phase formation, some contradictory results are found in the literature. Cook and Harper [21,22] report no  $\beta$  phase formation in either untreated and silane-treated  $Mg(OH)_2$  filled PP, while Liauw et al. [23] found  $\beta$ -phase in PP filled with  $Al(OH)_3$  surface-treated with 2-dodecen-1-yl succinic anhydride (DDSA).

Taking into account the previous information, it is possible to rationalise the former results. Firstly, due to the intense nucleating effect for PP  $\alpha$ -phase shown by the uncoated fillers [14,15], it seems logical that composites with these fillers do not develop PP  $\beta$ -modification. Secondly, it is less probable the presence of the  $\beta$ -phase in T specimens because the cooling rate is lower far away from the mould entrance than close to it. Furthermore, both the shear stress and cooling rate into the mould are much higher near the mould surface than in the core; consequently at the surface the material could reach the critical temperature ( $140^\circ C$ ) before the  $\alpha$ -phase has completed its

Table 4  
Intensity value of PP  $\beta$ -phase WAXD signal

Sample	LS	LP	TS	TP
<i>I</i> (300)				
PP	1493	837	–	–
PPH5	–	–	–	–
PPH5L	316	447	229	221
PPHKV	430	425	294	292
PPOL	w.s.	w.s.	–	–
PPON	w.s.	w.s.	–	–

w.s.—‘weak signal’, which could not be accurately quantified.

crystallisation. So, the  $\beta$ -phase could start growing and be detected in the WAXD scans taken from the surface. Nevertheless, only results of specimens L of unfilled PP confirm this hypothesis.

#### 4.2. Anisotropy and heterogeneity

To quantify the anisotropy resultant from orientation differences between the skin and the core of the specimens, the anisotropy degree concerning the filler particle effect (PAD) and the anisotropy degree concerning the polymer crystal (CAD) were calculated. The equations to calculate the particle anisotropy degree (PAD) in samples filled with  $Mg(OH)_2$  and  $Al(OH)_3$  have been, respectively:

$$PAD = \frac{(I(001)/I(101))_S - (I(001)/I(101))_P}{(I(001)/I(101))_S} \times 100 \quad (3)$$

$$PAD = \frac{(I(004)/I(110))_S - (I(004)/I(110))_P}{(I(004)/I(110))_S} \times 100 \quad (4)$$

And the equation to calculate the polymer crystal anisotropy degree (CAD) in all the samples:

$$CAD = \frac{(I(040)/I(110))_S - (I(040)/I(110))_P}{(I(040)/I(110))_S} \times 100 \quad (5)$$

Values of PAD are shown in Fig. 6(a). The three materials based on  $Mg(OH)_2$  present high values of the PAD parameter, therefore a high anisotropy regarding the particle orientation is expected. The two materials produced from PP and  $Al(OH)_3$  present lower values, especially interesting

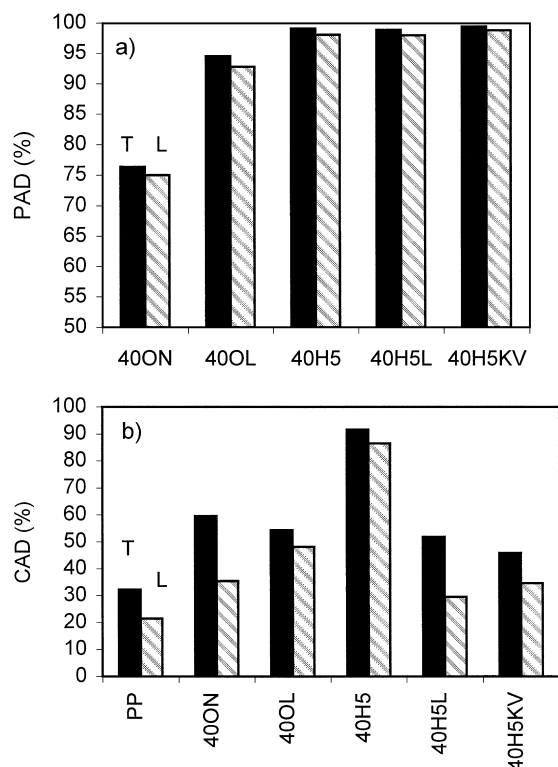


Fig. 6. (a) PAD and (b) CAD parameter for all the materials under study.

is the ON material, which shows the lowest values. This result should be connected to the particle morphology for this composite. As it was noted before, ON particles are coarse, and they can be considered as pseudo-spherical or globular ones as a result of irregular crystalline growing or aggregation of individual particles, unlike OL grade, which has finer and even some platy particles. So, ON particles would provoke lesser anisotropy than well-defined platy ones. This could be the reason for what PPOL samples result in intermediate values of PAD between those of platy  $Mg(OH)_2$  filled PP and those of filled with coarse  $Al(OH)_3$ .

In addition, the values of PAD in the T samples were always slightly higher than in the L ones. Due to the larger melt flow path during the mould filling, T specimens should have higher anisotropy (*S/P* differences) than L ones, as the results seem to indicate. As higher the flow path, higher particle orientation at the skin and higher anisotropy.

Values of CAD can be observed in Fig. 6(b). The filled materials have higher anisotropy concerning to the polymer crystal than the non-filled material. The PPH5 composite shows the highest values, which should be related to the higher nucleation activity for this composite [15] and as consequence to the greater influence of the particle orientation on the PP crystallisation. As it can be observed in this figure, the two surface treatments used reduce the orientation of the PP crystalline phase. Moreover, the two composites based on aluminium hydroxide present intermediate values between the values of unfilled PP and those of the PPH5 composite. Finally, it can be affirmed that the differences of the anisotropy degree between T and L specimens are higher in terms of polymer crystal orientation (CAD values) than in terms of filler particle orientation (PAD values).

In Fig. 7 the CAD parameter has been related to the PAD one. The effect of the surface treatments and particle morphology can be recognised clearly in this illustrative plot. On the one hand, the particle orientation effect remains constant when surface treatments are utilised, however these treatments seem to reduce the effect of the polymer orientation on the material anisotropy. On the other hand, the particle morphology has an influence on its orientation,

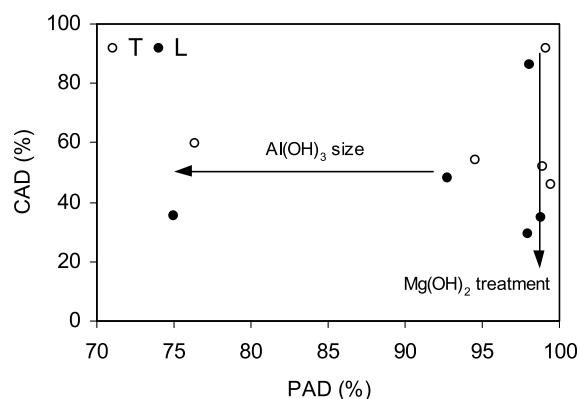


Fig. 7. Dependency between PAD and CAD parameters.

but the orientation of the polymeric matrix remains constant.

## 5. Conclusions

The fillers under study have induced different levels of interaction between their surface and the PP phase. As a consequence, different molecular immobilisation degrees have been detected in the molten-state, through the MFI-v values, and in the solid state through HDT values.

Injection-moulding discs had an anisotropic structure. On the one hand, filler platy particles were found mainly parallel to the disc surface in the skin zone. The kind of filler, its surface coating and its morphology influenced on the particle orientation, and as a consequence on the part anisotropy. On the other hand, the polymer crystalline phase also shown anisotropic structure, especially for materials filled with untreated minerals. There was no correlation between particle orientation and PP orientation. Furthermore, the PP  $\beta$ -phase could be detected in the L specimens of pure PP and in samples (L and T) of materials filled with surface-coated magnesium hydroxide.

The heterogeneity of the discs have also been considered and characterised in terms of filler particles and polymer orientations. All the filled materials presented a similar degree of heterogeneity. The samples far away from the mould entrance had a more pronounced particles orientation, probably due to the flow restriction that the melt suffers as it progress in the mould cavity.

## Acknowledgements

The authors thank to MCYT (Government of Spain) for the financial assistance of the project MAT 2000-1112. Also, C. Morhain thanks to CIRIT (Government of Catalonia, Spain), the concession of a predoctoral grant.

## References

- [1] Katz HS, Milewsky JV. Handbook of fillers and reinforcement for plastics. New York: Van Nostrand Reinhold; 1978.
- [2] Velasco JI, de Saja JA, Martínez AB. J Appl Polym Sci 1996;61: 125–32.
- [3] Velasco JI, de Saja JA, Martínez AB. Fatigue Fract Engng Mater Struct 1997;20:659–70.
- [4] Xavier SF, Schultz JM, Friedrich K. J Mater Sci 1990;25:2411–20.
- [5] Xavier SF, Schultz JM, Friedrich K. J Mater Sci 1990;25:2421–7.
- [6] Xavier SF, Schultz JM, Friedrich K. J Mater Sci 1990;25:2428–32.
- [7] Fujiyama M. Higher order structure of injection-moulded polypropylene. In: Karger-Kocsis J, editor. Polypropylene: structure, blends and composites, vol. 1. London: Chapman & Hall; 1995. p. 167–204.
- [8] Fujiyama M, Wakino T. J Appl Polym Sci 1991;42:2739–47.
- [9] Fujiyama M. Int Polym Process 1992;7:165–71.
- [10] Gilbert M, Sutherland I, Guest A. J Mater Sci 2000;35:391–7.
- [11] Pukánszky B. Particulate filled polypropylene: structure and properties. In: Karger-Kocsis J, editor. Polypropylene: structure, blends and composites, vol. 3. London: Chapman & Hall; 1995. p. 1–70.
- [12] Haworth B, Gilbert M, Raymond CL. J Mater Sci Lett 2000;19: 1415–8.
- [13] Díez-Gutiérrez S, Rodríguez-Pérez MA, de Saja JA, Velasco JI. Polymer 1999;40:5345–53.
- [14] Velasco JI, Morhain C, Martínez AB, Rodríguez-Pérez MA, de Saja JA. Macromol Mater Engng 2001;286:719–30.
- [15] Velasco JI, Morhain C, Martínez AB, Rodríguez-Pérez MA, de Saja JA. Polymer 2002;43:6813–9.
- [16] Kumaraswamy G, Verma RK, Issaian AM, Wang P, Kornfield JA, Yeh F, Hsiao BS, Olley RH. Polymer 2000;41:8931–40.
- [17] Addink EJ, Beintema J. Polymer 1961;2:185–93.
- [18] Rybnikar F. J Appl Polym Sci 1989;38:1479–90.
- [19] Varga J. Crystallization, melting and supermolecular structure of isotactic polypropylene. In: Karger-Kocsis J, editor. Polypropylene: structure, blends and composites, vol. 1. London: Chapman & Hall; 1995. p. 56–115.
- [20] Shi G, Chu F, Zhou G, Han Z. Makromol Chem 1989;190:907–13.
- [21] Cook M, Harper JF. Plast, Rubber Compos Process Appl 1996;25: 99–105.
- [22] Cook M, Harper JF. Adv Polym Technol 1998;17:53–62.
- [23] Liauw CM, Lees GC, Hurst SJ, Rothern RN, Dobson DC. Angew Makromol Chem 1996;235:193–203.